APPLIED PHYSICS LETTERS 111, 043110 (2017)

Large array fabrication of high performance monolayer MoS_2 photodetectors

Alexander E. Yore,[1,a)] Kirby K. H. Smithe,[2,a)] Sauraj Jha,[1] Kyle Ray,[1] Eric Pop,[2,3,4] and A. K. M. Newaz[1]

[1]*Department of Physics and Astronomy, San Francisco State University, San Francisco, California 94132, USA*
[2]*Department of Electrical Engineering, Stanford University, Stanford, California 94305, USA*
[3]*Department of Materials Science and Engineering, Stanford University, Stanford, California 94305, USA*
[4]*Precourt Institute for Energy, Stanford University, Stanford, California 94305, USA*

(Received 24 March 2017; accepted 13 July 2017; published online 28 July 2017)

Large array fabrication of high quality photodetectors derived from synthetically grown monolayer transition metal dichalcogenides is highly desired and important for a wide range of nanophotonic applications. We present here large array fabrication of monolayer MoS_2 photodetectors on sapphire substrates through an efficient process, which includes growing large scale monolayer MoS_2 via chemical vapor deposition (CVD) and multi-step optical lithography for device patterning and high quality metal electrode fabrication. In every measured device, we observed the following universal features: (i) negligible dark current ($I_{dark} \leq 10$ fA), (ii) sharp peaks in photocurrent at $\sim$1.9 eV and $\sim$2.1 eV attributable to the optical transitions due to band edge excitons, and (iii) a rapid onset of photocurrent above $\sim$2.5 eV peaked at $\sim$2.9 eV due to an excitonic absorption originating from the van Hove singularity of MoS_2. We observe a low ($\leq$300%) device-to-device variation of photoresponsivity. Furthermore, we observe a very fast DC time response of $\sim$0.5 ms, which is two orders of magnitude faster than other reported CVD grown 1L-MoS_2 based photodetectors. The combination of large-array device fabrication, high sensitivity, and high speed offers great potential for applications in photonics. *Published by AIP Publishing.*
[http://dx.doi.org/10.1063/1.4995984]

Atomically thin monolayer (1L) two-dimensional (2D) transition-metal dichalcogenides (TMDs) are attractive materials for next-generation nanoscale optoelectronic applications and have gained tremendous interest in a wide range of fields.[1–4] TMDs demonstrate several extraordinary properties that make them very attractive for optical, electrical, and opto-electronic applications. First, 2D confinement, direct band-gap nature,[5] a large surface-to-volume ratio,[6] and weak screening of charge carriers enhance light-matter interactions[5,7–10] in these materials which lead to extraordinarily high absorption. Second, strong light-matter interactions create electron-hole (*e-h*) pairs and form two-body bound states, known as excitons (a hydrogenic entity made of an *e-h* pair).[11–16] Furthermore, 1L-TMDs are compatible with the complementary metal-oxide semiconductor (CMOS) industry,[17] as well as chemical, thermal, and pressure stability.[18] However, most of the opto-electrical prototypes involving 2D layered TMDs have been obtained either via mechanical exfoliation of 1L-TMDs from bulk crystals[2,11] or using chemical vapor deposition (CVD) grown single flakes.[19,20] To advance technology, establishing processes to fabricate large arrays of TMD based devices with homogeneous size and architecture is of utmost interest, not only from the scalability point of view but also to ensure a low device-to-device variability. Here, we demonstrate large-array fabrication of photodetectors based on CVD grown MoS_2 and their intrinsic optoelectronic behavior. We observed negligibly small dark current ($I_{dark} \leq 10$ fA), high photocurrent (PC) responsivity ($\sim$1 mA/W) for UV photons ($\sim$400 nm), and fast DC photoresponse time ($\sim$0.5 ms) which is two orders magnitude faster than that of other CVD grown 1L-MoS_2 based photodetectors.[21,22] Our devices demonstrate a low device-to-device variation of photoresponsivity ($\leq$300%). Our study provides a fundamental understanding of these devices and may lead to important nanophotonic device development with tailored characteristics.

Large-scale growth of uniform 1L-MoS_2 is performed using solid S and MoO_3 precursors directly onto optically inactive ($300\,\text{nm} \leq \lambda \leq 700\,\text{nm}$) sapphire substrates following a method similar to that previously reported by Dumcenco *et al.*[23] The growth process is optimized to obtain complete coverage of a large sample (1 cm $\times$ 1 cm). The layer thickness of the grown sample is subsequently confirmed by Raman and photoluminescence spectroscopy[24–27] and atomic force microscopy (AFM) as shown in Figs. 1(a) and 1(b). After growth, three steps of optical lithography are conducted to define device dimensions and obtain a low contact resistance.[54] First, large contact pads (2/40 nm of Ti/Au) are patterned via optical lithography, etching away MoS_2 with O_2 plasma, metal evaporation, and liftoff. Second, Ag (contact layer)/Au (25/25 nm) contacts are fabricated in a similar fashion, omitting the plasma etch. Finally, the channel is defined via similar optical lithography and O_2 plasma etching. The optical image of an array of devices is shown in Fig. 1(c) along with a high resolution image of one device as in Fig. 1(d). The metal contact area is marked by a dashed trapezoid in Fig. 1(d). The fluorescence image (excitation $\sim$405 nm) confirming the presence of a 1L-MoS_2 ribbon (marked by a white dashed rectangular box) is shown in Fig. 1(e). We fabricated samples with varying lengths and widths. Here, we

[a)]A. E. Yore and K. K. H. Smithe contributed equally to this work.

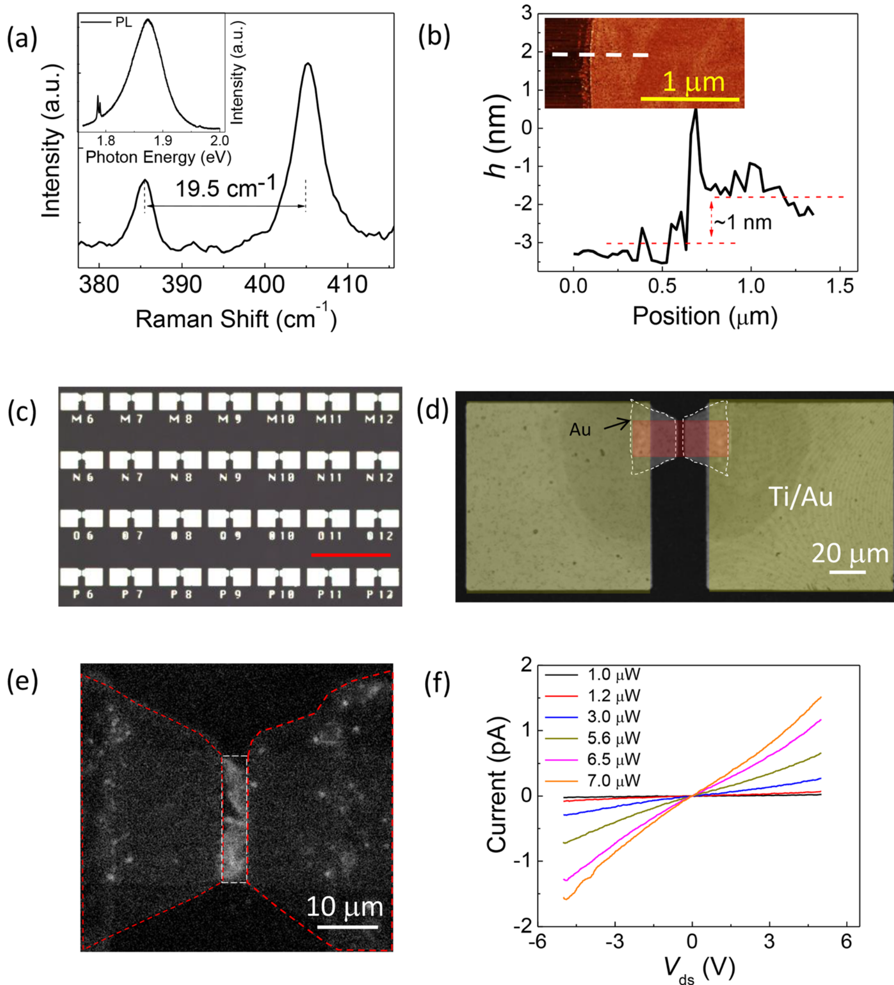

FIG. 1. Sample characterization and *I-V* behavior. (a) Raman spectrum of a sample with a 532 nm excitation laser. Inset: photoluminescence spectrum of the sample (excitation laser wavelength, $\lambda \sim 532$ nm). The doublet peaks around $\sim$1.79 eV originate from the sapphire substrate. (b) The line profile of the device channel measured by an AFM. The AFM image is shown in the inset. The line profile is taken along the dashed white line. (c) An array of photodetectors. The bright squares shows the Ti/Au (2/40 nm) bonding pads. The scale bar (red solid line) is 400 μm. (d) False-colored and high resolution optical image of a device. The 1L-MoS_2 etched ribbon is marked by a red rectangle. The Ag/Au (25/25 nm) electrical connection to the sample is marked by a dashed trapezoid. (e) The fluorescence image of a device. The fluorescing 1L-MoS_2 sample in the middle (marked by the white dashed rectangle) confirms the presence of the flake between the electrodes. The metal contact area is shown by a trapezoid (red dashed line). The sample was excited by a blue laser ($\lambda \sim 405$ nm). (f) I-V curves for different laser powers ($\lambda \sim 405$ nm laser). All the measurements were carried out at room temperature in ambient conditions.

are presenting the electrical and electro-optical data for the devices with a length of 2 μm and a width of 20 μm. All the measurements were conducted at room temperature and in ambient conditions.

First, we discuss the electrical transport measurements. We observed zero dark current within our measurement capabilities ($\sim$10 fA). On the other hand, the sample demonstrated conducting behavior while pumped by a blue laser ($\sim$405 nm). The laser power dependent *I-V* curve is shown in Fig. 1(f). The blue laser beam diameter was $\sim$2 μm. The insulating behavior in the dark suggests that the 1L-MoS_2 ribbons are undoped, and the Fermi level resides in the band gap.[28] This also suggests that the substrate is not introducing any charge impurities to dope the sample.[28] The observed conducting behavior of the sample when impinged upon by a laser is due to the creation of photocarriers, which dope the system, a process known as optical doping.[29] To understand the doping nature of our sample, we conducted power resolved photocurrent measurements discussed below.

The superlinear behavior of the *I-V* curve suggests that the Ag/Au metal contact with MoS_2 forms Schottky barriers, similar to the results demonstrated earlier by Yuan *et al.*[30] and Liu *et al.*[31] Hence, our photodetectors are metal-semiconductor-metal (MSM) photodetectors with two Schottky barriers connected back-to-back on a coplanar surface.[32]

Now, we focus on the wavelength resolved photocurrent measurements. We measured photocurrent (PC) responsivity (PC per unit power) to explore different two-body excitons in 1L-MoS_2. We illuminate the entire device using a low intensity broadband white light ($P_{tot} \sim 20$ pW/μm^2) from a thermal light source and record photocurrent I_{PC} across the device as a function of the photon energy $\hbar\omega$. The photocurrent was measured by using a lock-in technique. The optical beam from a broadband thermal source (quartz halogen lamp) was guided through a monochromator (Acton Pro SP-2150i) and a mechanical chopper ($\sim$40 Hz) onto the sample where it was focused down to a spot with a diameter of $\sim$75 μm. To calibrate the light intensity at the sample, the intensity of the beam was recorded by using a Si detector (Thorlabs DET10A). We measured PC under high V_{ds} ($\geq$5 V) [Fig. 2(a)]. We observe several major characteristics: (i) two sharp peaks at $\sim$1.9 eV and $\sim$2.1 eV (labeled "*A*" and "*B*," respectively, as they originate from *A*- and *B*-excitons[28]), (ii) steep growth of PC starting at $\sim$2.5 eV, and (iii) a broad and strong peak "*C*" at $\sim$2.9 eV. We note that the high photosensitivity of our 1L-MoS_2 phodetectors allowed us to use very low illumination intensity in our experiments. Low power density is beneficial for the excitonic photocurrent measurement as it excludes photo-thermoelectric effects[33] and optically non-linear[34] effects arising at high photocarrier densities.

Features *A* and *B* in the PC spectrum arise from the neutral excitons formed by direct *A* and *B* excitonic transitions across the band gap.[28,35,36] The large peak in the UV regime is known as the *C*-peak, which is associated with the van Hove singularity (*vHS*) excitons.[28,37] This *vHS* is extraordinary in nature as both the conduction band, and the valence

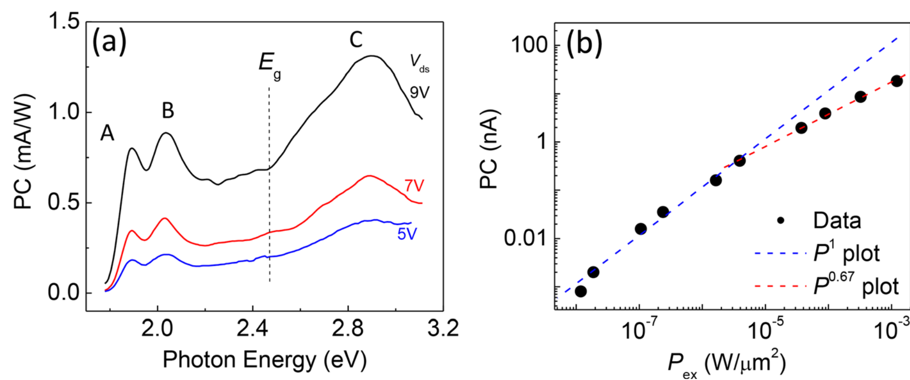

FIG. 2. (a) Photocurrent spectrum for different drain-source voltages; 5 V (blue), 7 V (red), and 9 V (black). Three peaks at 1.9 eV, 2 eV, and 2.9 eV are identified as the *A*, *B*, and *C* peaks. The sharp rise of PC at 2.5 eV is associated with the band edge transition, i.e., the direct transition between the valence maxima and the conduction band minima ($\sim E_g$). (b) The photocurrent with varying laser ($\lambda \sim 405$ nm) excitation powers (P_{ex}) measured for $V_{ds} = 1$ V. The dashed lines indicate the power law ($\boldsymbol{I_{PC} \propto P^{\alpha}}$) fitting (see text). The blue and red dashed lines are drawn for $\alpha \sim 1$ and ~ 0.67, respectively.

band do not have singularities in the electronic density of states in the corresponding region of the Brillouin zone (BZ).[28,37] However, near the Γ point of the BZ, the conduction and valence bands are locally parallel, which creates a Mexican hat-like potential in the optical band structure (~CB-VB_A, where CB and VB_A are the conduction band and the upper valence band, respectively). Hence, the optical joint density of states at the bottom of the Mexican hat potential diverges creating the *vHS* singularity. That is why the *C*-peak demonstrates an extraordinarily high absorption coefficient for 1L-MoS_2 (~40%).[7,37,38] Since these singularity assisted excitons reside in the continuum above the band-edge, these excitons dissociate spontaneously and may have very short lifetimes, which can be utilized to develop ultrafast UV photodetectors. Recently, we reported recently similar characteristics obtained for the suspended pristine 1L-MoS_2 sample prepared by micro-exfoliation from bulk crystals.[28]

To explore the defects of the 1L-MoS_2 sample on sapphire substrates, we conducted laser power (P_{ex}) resolved PC measurements. Figure 2(b) shows the power dependence of the PC for $V_{ds} = 1$ V. The dependence follows a power law, $I_{PC} \propto P^{\alpha}$, where P is the laser power. To study the photoresponse effect originating from the van Hove singularity excitons, the sample was pumped by a blue laser (~405 nm). We observed a linear behavior in the low power regime ($P \leq 4\,\mu W/\mu m^2$) and sublinear behavior with $\alpha \sim 0.67$ for a higher power range ($P \geq 4\,\mu W/\mu m^2$). This sublinear power behavior can be attributed to several causes: (i) saturable absorption (phase space filling);[39–41] (ii) photogenerated carriers recombine via MoS_2 defects and charge impurities around MoS_2;[20] (iii) electron-hole recombination;[42] (iv) exciton-exciton annihilation;[43,44] and (v) carrier-carrier scattering.[40] A similar sublinear power law for MoS_2 has been reported recently[39,45] and observed for other semiconductor based photodetectors.[46,47]

To demonstrate the device performance variation, we present the photoresponsivity curves for ten different devices as shown in Fig. 3(a). All the measurements were conducted under the same optical and electrical settings in ambient air. We found that the maximum responsivity at $\lambda \sim 450$ nm varies by ~300% from the lowest values as shown in Fig. 3(a) or the variation of photoresponsivity all the devices falls within ~50% of the average value. We observed 100% variations in the PL spectrum and almost no variations in the Raman spectrum (see the supplementary material).

Finally, we discuss the time-response behavior of our devices for UV photons (~405 nm) shown in Figs. 3(b) and 3(c). Since the laser excitation energy is ~3 eV (405 nm), the PC response in our samples originates from the "*C*" *vHS* excitons. There are two different types of time-response measurement available: (i) DC time response by measuring the time variation directly using a high speed oscilloscope and (ii) AC time response by employing a lock-in amplifier.[48] Here, we report the DC time response, by measuring the photocurrent signal variation employing a high speed oscilloscope (Tektronix TDS 380) as we block and unblock the

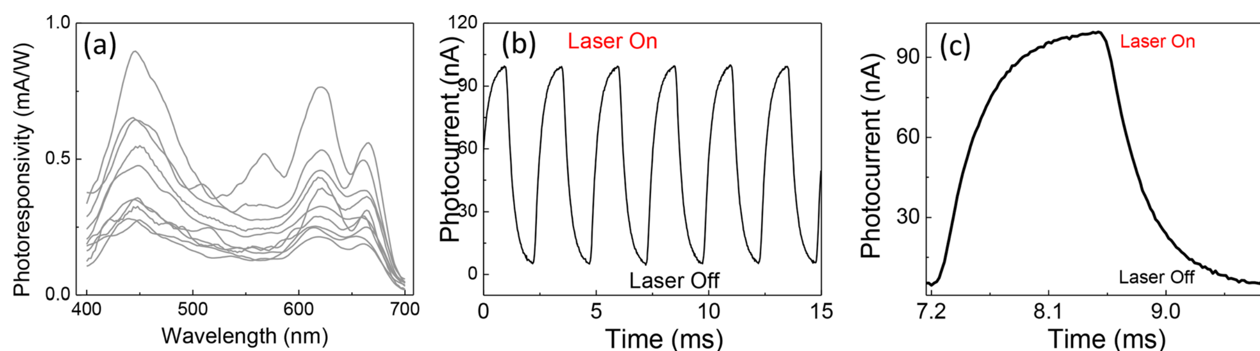

FIG. 3. Photoresponsivity variations and the time-response behavior of the 1L-MoS_2 photodetector. (a) The photoresponsivity of ten different samples measured in ambient conditions. (b) The photocurrent response as the laser was modulated by a mechanical chopper. The excitation laser wavelength was ~405 nm. (c) Enhanced view of a single PC pulse. The rise time (0%–90%) was 0.5 ms, and the drop-off time was 0.8 ms.

laser beam. Figure 3(b) presents PC as the laser is chopped by a mechanical wheel with a chopping frequency of ~400 Hz. The excitation power was ~100 μW. Figure 3(c) shows the blow up view of one PC pulse. We observed a very fast DC rise time (0%–90%) of ~0.5 ms, suggesting that our current device will function at a speed of ~2 kHz.

We attribute the fast photoresponse of our devices to two possible reasons. First, the devices were prepared on an optically transparent substrate, sapphire. Second, we connected the 1L-MoS_2 flakes via Ag (contact layer)/Au electrodes, which causes a lower contact resistance.[30] Commonly, TMD devices are prepared on SiO_2/Si substrates to elucidate the gate dependent transport properties. However, the electronic band bends at the interface of SiO_2/Si that creates a quantum well causing photo-voltage or photogating.[48,49] The optical photon with energy larger than Si band-gap ($\lambda \leq 1130$ nm) creates photogenerated electron-hole pairs in the doped Si substrate. The quantum well at the interface traps either electrons or holes, which causes photovoltage.[50] To avoid the effect of the photovoltage or photogating on the optoelectronic behavior of our samples, we have grown 1L-MoS_2 via CVD on sapphire.

Significant progress has been made in studying the photoresponse behaviors in a wide range of TMDs, and readers are referred to review articles.[21,51] For TMD based optoelectronic devices, the fastest DC photoresponse ($\tau \sim 5$ ps) is observed in devices derived from exfoliated 1L-MoS_2[52] and multilayer WSe_2.[53] For CVD grown 1L-MoS_2 and 1L-WSe_2 devices, the fastest DC photoresponse reported values are ~55 ms (Ref. 22) and ~23 ms,[53] respectively. Hence, the DC time response in our 1L-MoS_2 based devices is ~100 times faster than other reported DC photoresponse values for CVD grown 1l-MoS_2 devices. Thus, our large array photodetectors demonstrate potentials for high speed photonic applications. We also note that Yang *et al.*[48] recently reported AC time constant to be ~3 ms for CVD grown 1L-MoS_2 devices.

In conclusion, we demonstrated large array fabrication of fast and ultra-sensitive photodetectors based on CVD grown 1L-MoS_2. We determined several important figures of merits for our devices: responsivity, time response, and scalability. Our results yield fundamental understanding of CVD-derived TMD devices and will provide important information to develop next generation TMD based nanophotonic devices.

See supplementary material for the photoluminescence and Raman spectrum for ten devices.

We thank Dr. Annette Chan for the help in performing the high resolution fluorescent imaging of the sample. A.K.M.N., S.J., K.R., and A.E.Y. are grateful for the financial support from SFSU. K.K.H.S. and E.P. acknowledge support from the AFOSR Grant No. FA9550-14-1-0251 and NSF EFRI 2-DARE Grant No. 1542883. K.K.H.S. also acknowledges partial support from the Stanford Graduate Fellowship program and NSF Graduate Research Fellowship under Grant No. DGE-114747. This research used the Cell and Molecular Imaging Center at SFSU. Parts of this work were also performed at the Stanford Nanofabrication Facility and Stanford Nano Shared Facilities.

[1] F. Xia, H. Wang, D. Xiao, M. Dubey, and A. Ramasubramaniam, Nat. Photonics **8**, 899 (2014).
[2] K. F. Mak and J. Shan, Nat. Photonics **10**, 216 (2016).
[3] K. S. Novoselov, A. Mishchenko, A. Carvalho, and A. H. Castro Neto, Science **353**, aac9439 (2016).
[4] X. Duan, C. Wang, A. Pan, R. Yu, and X. Duan, Chem. Soc. Rev. **44**, 8859 (2015).
[5] K. F. Mak, C. Lee, J. Hone, J. Shan, and T. F. Heinz, Phys. Rev. Lett. **105**, 136805 (2010).
[6] S. Yang, S. Tongay, Q. Yue, Y. Li, B. Li, and F. Lu, Sci. Rep. **4**, 5442 (2014).
[7] L. Britnell, R. M. Ribeiro, A. Eckmann, R. Jalil, B. D. Belle, A. Mishchenko, Y.-J. Kim, R. V. Gorbachev, T. Georgiou, S. V. Morozov, A. N. Grigorenko, A. K. Geim, C. Casiraghi, A. H. Castro Neto, and K. S. Novoselov, Science **340**, 1311 (2013).
[8] A. Splendiani, L. Sun, Y. Zhang, T. Li, J. Kim, C.-Y. Chim, G. Galli, and F. Wang, Nano Lett. **10**, 1271 (2010).
[9] X. Liu, T. Galfsky, Z. Sun, F. Xia, E.-C. Lin, Y.-H. Lee, S. Kéna-Cohen, and V. M. Menon, Nat. Photonics **9**, 30 (2015).
[10] W. J. Yu, Y. Liu, H. Zhou, A. Yin, Z. Li, Y. Huang, and X. Duan, Nat. Nanotechnol. **8**, 952 (2013).
[11] O. Lopez-Sanchez, D. Lembke, M. Kayci, A. Radenovic, and A. Kis, Nat. Nanotechnol. **8**, 497 (2013).
[12] Q. H. Wang, K. Kalantar-Zadeh, A. Kis, J. N. Coleman, and M. S. Strano, Nat. Nanotechnol. **7**, 699 (2012).
[13] B. W. H. Baugher, H. O. H. Churchill, Y. Yang, and P. Jarillo-Herrero, Nat. Nanotechnol. **9**, 262 (2014).
[14] G. Eda and S. A. Maier, ACS Nano **7**, 5660 (2013).
[15] J. S. Ross, P. Klement, A. M. Jones, N. J. Ghimire, J. Yan, D. G. Mandrus, T. Taniguchi, K. Watanabe, K. Kitamura, W. Yao, D. H. Cobden, and X. Xu, Nat. Nanotechnol. **9**, 268 (2014).
[16] R. S. Sundaram, M. Engel, A. Lombardo, R. Krupke, A. C. Ferrari, P. Avouris, and M. Steiner, Nano Lett. **13**, 1416 (2013).
[17] H. Liu, J. J. Gu, and P. D. Ye, IEEE Electron Device Lett. **33**, 1273 (2012).
[18] N. Bandaru, R. S. Kumar, D. Sneed, O. Tschauner, J. Baker, D. Antonio, S.-N. Luo, T. Hartmann, Y. Zhao, and R. Venkat, J. Phys. Chem. C **118**, 3230 (2014).
[19] N. Perea-Lopez, Z. Lin, N. R. Pradhan, A. Iniguez-Rabago, A. L. Elias, A. McCreary, J. Lou, P. M. Ajayan, H. Terrones, L. Balicas, and M. Terrones, 2D Mater. **1**, 011004 (2014).
[20] W. Zhang, J.-K. Huang, C.-H. Chen, Y.-H. Chang, Y.-J. Cheng, and L.-J. Li, Adv. Mater. **25**, 3456 (2013).
[21] Q. S. Wang, J. W. Lai, and D. Sun, Opt. Mater. Express **6**, 2313 (2016).
[22] X. Yang, Q. Li, G. Hu, Z. Wang, Z. Yang, X. Liu, M. Dong, and C. Pan, Sci. China Mater. **59**, 182 (2016).
[23] D. Dumcenco, D. Ovchinnikov, K. Marinov, P. Lazić, M. Gibertini, N. Marzari, O. L. Sanchez, Y.-C. Kung, D. Krasnozhon, M.-W. Chen, S. Bertolazzi, P. Gillet, A. Fontcuberta i Morral, A. Radenovic, and A. Kis, ACS Nano **9**, 4611 (2015).
[24] H. Li, Q. Zhang, C. C. Ray Yap, B. K. Tay, T. H. Tong Edwin, A. Olivier, and D. Baillargeat, Adv. Funct. Mater. **22**, 1385 (2012).
[25] X. Zhang, X.-F. Qiao, W. Shi, J.-B. Wu, D.-S. Jiang, and P.-H. Tan, Chem. Soc. Rev. **44**, 2757 (2015).
[26] C. Lee, H. Yan, L. E. Brus, T. F. Heinz, J. Hone, and S. Ryu, ACS Nano **4**, 2695 (2010).
[27] A. M. van der Zande, P. Y. Huang, D. A. Chenet, T. C. Berkelbach, Y. You, G.-H. Lee, T. F. Heinz, D. R. Reichman, D. A. Muller, and J. C. Hone, Nat. Mater. **12**, 554 (2013).
[28] A. R. Klots, A. K. M. Newaz, B. Wang, D. Prasai, H. Krzyzanowska, J. Lin, D. Caudel, N. J. Ghimire, J. Yan, B. L. Ivanov, K. A. Velizhanin, A. Burger, D. G. Mandrus, N. H. Tolk, S. T. Pantelides, and K. I. Bolotin, Sci. Rep. **4**, 6608 (2014).
[29] H. S. Lee, M. S. Kim, H. Kim, and Y. H. Lee, Phys. Rev. B **93**, 140409 (2016).
[30] H. Yuan, G. Cheng, L. You, H. Li, H. Zhu, W. Li, J. J. Kopanski, Y. S. Obeng, A. R. Hight Walker, D. J. Gundlach, C. A. Richter, D. E. Ioannou, and Q. Li, ACS Appl. Mater. Interfaces **7**, 1180 (2015).
[31] H. Liu, M. Si, Y. Deng, A. T. Neal, Y. Du, S. Najmaei, P. M. Ajayan, J. Lou, and P. D. Ye, ACS Nano **8**, 1031 (2014).
[32] S. M. Sze and K. K. Ng, *Physics of Semiconductor Devices*, 3rd ed. (Wiley-Interscience, Hoboken, NJ, 2007), p. 712.
[33] M. Buscema, M. Barkelid, V. Zwiller, H. S. J. van der Zant, G. A. Steele, and A. Castellanos-Gomez, Nano Lett. **13**, 358 (2013).
[34] D. S. Chemla and J. Shah, Nature **411**, 549 (2001).

[35]K. F. Mak, K. He, C. Lee, G. H. Lee, J. Hone, T. F. Heinz, and J. Shan, Nat. Mater. **12**, 207 (2013).
[36]D. Xiao, G. B. Liu, W. X. Feng, X. D. Xu, and W. Yao, Phys. Rev. Lett. **108**, 196802 (2012).
[37]D. Y. Qiu, F. H. da Jornada, and S. G. Louie, Phys. Rev. Lett. **111**, 216805 (2013).
[38]C. Zhang, H. Wang, W. Chan, C. Manolatou, and F. Rana, Phys. Rev. B **89**, 205436 (2014).
[39]M. Massicotte, P. Schmidt, F. Vialla, K. G. Schädler, A. Reserbat Plantey, K. Watanabe, T. Taniguchi, K. J. Tielrooij, and F. H. L. Koppens, Nat. Nanotechnol. **11**, 42 (2016).
[40]Z. Nie, R. Long, L. Sun, C.-C. Huang, J. Zhang, Q. Xiong, D. W. Hewak, Z. Shen, O. V. Prezhdo, and Z.-H. Loh, ACS Nano **8**, 10931 (2014).
[41]K. Wang, J. Wang, J. Fan, M. Lotya, A. O'Neill, D. Fox, Y. Feng, X. Zhang, B. Jiang, Q. Zhao, H. Zhang, J. N. Coleman, L. Zhang, and W. J. Blau, ACS Nano **7**, 9260 (2013).
[42]N. M. Gabor, Z. Zhong, K. Bosnick, and P. L. McEuen, Phys. Rev. Lett. **108**, 087404 (2012).
[43]S. Mouri, Y. Miyauchi, M. Toh, W. Zhao, G. Eda, and K. Matsuda, Phys. Rev. B **90**, 155449 (2014).
[44]D. Sun, Y. Rao, G. A. Reider, G. Chen, Y. You, L. Brézin, A. R. Harutyunyan, and T. F. Heinz, Nano Lett. **14**, 5625 (2014).
[45]C.-C. Wu, D. Jariwala, V. K. Sangwan, T. J. Marks, M. C. Hersam, and L. J. Lauhon, J. Phys. Chem. Lett. **4**, 2508 (2013).
[46]J. Lähnemann, M. Den Hertog, P. Hille, M. de la Mata, T. Fournier, J. Schörmann, J. Arbiol, M. Eickhoff, and E. Monroy, Nano Lett. **16**, 3260 (2016).
[47]F. González-Posada, R. Songmuang, M. Den Hertog, and E. Monroy, Nano Lett. **12**, 172 (2012).
[48]Z. Yang, R. Grassi, M. Freitag, Y.-H. Lee, T. Low, and W. Zhu, Appl. Phys. Lett. **108**, 083104 (2016).
[49]M. S. Marcus, J. M. Simmons, O. M. Castellini, R. J. Hamers, and M. A. Eriksson, J. Appl. Phys. **100**, 084306 (2006).
[50]M. Freitag, T. Low, F. Xia, and P. Avouris, Nat. Photonics **7**, 53 (2013).
[51]M. Buscema, J. O. Island, D. J. Groenendijk, S. I. Blanter, G. A. Steele, H. S. J. van der Zant, and A. Castellanos-Gomez, Chem. Soc. Rev. **44**, 3691 (2015).
[52]H. N. Wang, C. J. Zhang, W. M. Chan, S. Tiwari, and F. Rana, Nat. Commun. **6**, 8831 (2015).
[53]W. Zhang, M.-H. Chiu, C.-H. Chen, W. Chen, L.-J. Li, and A. T. Shen Wee, ACS Nano **8**, 8653 (2014).
[54]K. K. H. Smithe, S. V. Suryavanshi, M. Munoz-Rojo, A. D. Tedjarati, and E. Pop, ACS Nano (to be published).

Large Array Fabrication of High Performance Monolayer MoS_2 Photodetectors

Alexander E. Yore[1,a)], K.K.H. Smithe[2, a)], Sauraj Jha[1], Kyle Ray[1], Eric Pop[2-4] and A.K.M. Newaz[1]

[1]Department of Physics and Astronomy, San Francisco State University, San Francisco, California 94132, U.S.A.

[2]Department of Electrical Engineering, Stanford University, Stanford, California 94305, U.S.A.

[3]Department of Materials Science and Engineering, Stanford University

[4]Precourt Institute for Energy, Stanford University

Variation of the photoluminescence and Raman spectrum for ten devices:

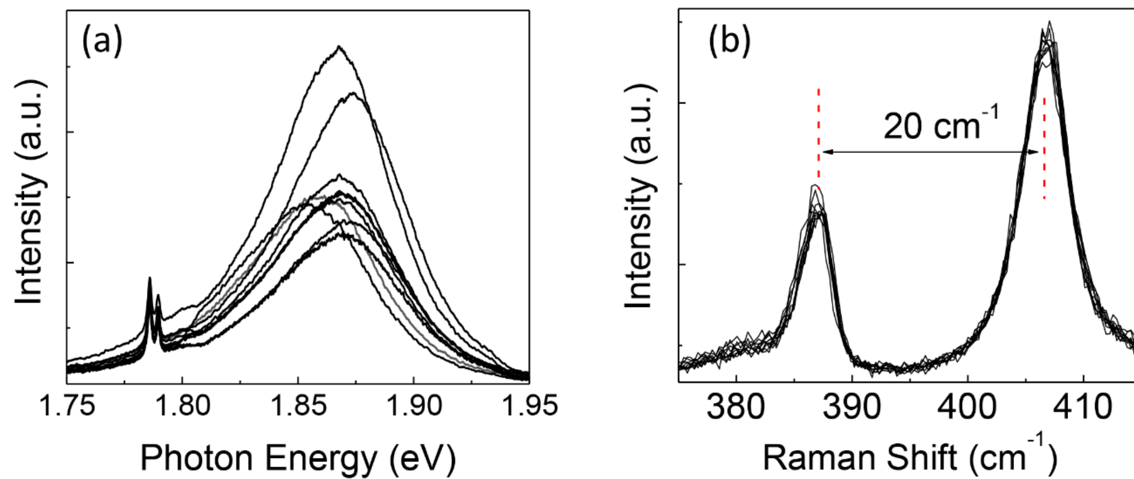

Figure S1: (a) and (b) are presenting the variations of the PL and Raman spectrum, respectively, for ten devices. The measurements were carried out in ambient condition. The excitation laser wavelength was 532 nm.